



Metabolic engineering of *Schizosaccharomyces pombe* for itaconic acid production

Fujie, Naofumi ; Ito, Miki ; Kishida, Mayumi ; Hirata, Yuuki ; Kondo, Akihiko ; Tanaka, Tsutomu

(Citation)

Journal of Biotechnology, 358:111-117

(Issue Date)

2022-11-10

(Resource Type)

journal article

(Version)

Accepted Manuscript

(Rights)

© 2022 Elsevier B.V.

This manuscript version is made available under the Creative Commons Attribution-NonCommercial-NoDerivatives 4.0 International license.

(URL)

<https://hdl.handle.net/20.500.14094/0100476961>



1 **Metabolic engineering of *Schizosaccharomyces pombe* for itaconic acid production**

2 Naofumi Fujie¹, Miki Ito¹, Mayumi Kishida¹, Yuuki Hirata¹, Akihiko Kondo^{2,3}, and Tsutomu Tanaka^{1*}

3 ¹Department of Chemical Science and Engineering, Graduate School of Engineering, Kobe University, 1-
4 1 Rokkodai, Nada, Kobe 657-8501, Japan

5 ²Center for Sustainable Resource Science, RIKEN, 1-7-22 Suehiro-cho, Tsurumi-ku, Yokohama, Kanagawa
6 230-0045, Japan

7 ³Graduate School of Science, Technology and Innovation, Kobe University, 1-1 Rokkodai, Nada, Kobe
8 657-8501, Japan

9 *Corresponding author: Tsutomu Tanaka, **Email:** tanaka@kitty.kobe-u.ac.jp

11 **Abstract**

12 The economical production of value-added chemicals from renewable biomass is a promising aspect of
13 producing a sustainable economy. Itaconic acid (IA) is a high value-added compound that is expected to be
14 an alternative to petroleum-based chemicals. In this study, we developed a metabolic engineering strategy
15 for the large-scale production of IA from glucose using the fission yeast *Schizosaccharomyces pombe*.
16 Heterologous expression of the *cis*-aconitic acid decarboxylase (CAD) gene from *Aspergillus terreus*,
17 which encodes *cis*-aconitate decarboxylase in the cytosol, led to the production of 0.132 g/L of IA. We
18 demonstrated that mitochondrial localization of CAD enhanced the production of IA. To prevent the leakage
19 of carbon flux from the TCA cycle, we generated a strain in which the endogenous malate exporter, citrate
20 lyase, and citrate transporter genes were disrupted. A titer of 1.110 g/L of IA was obtained from a culture
21 of this strain started with 50 g/L of glucose. By culturing the multiple mutant strain at increased cell density,
22 we succeeded in enhancing the IA production to 1.555 g/L. The metabolic engineering strategies presented
23 in this study have the potential to improve the titer of the biosynthesis of derivatives of intermediates of the
24 TCA cycle.

25 **Keywords** Itaconic acid, *Schizosacchchromyces pombe*, Metabolic engineering, Mitochondria

Highlights

- *Schizosaccharomyces pombe* producing itaconic acid was constructed.
- Mitochondrial localization of CAD improved itaconic acid production.
- The highest itaconic acid production used *S. pombe* as a host.

1. Introduction

In order to meet the growing worldwide interest in sustainability, we need to develop eco-friendly technologies. Microbial fermentation, a process used to produce commodity and specialty chemicals from renewable raw materials, using microorganisms, is an innovative solution to this challenge. In a report from the US Department of Energy (DOE) in 2004, itaconic acid (IA) was selected as one of the most valuable chemicals which can be produced from biomass (Werpy et al., 2004). IA is a highly reactive dicarboxylic acid that is used as a precursor for a variety of organic compounds, such as food additives and medicines. IA can also be used as a co-monomer for super-absorbent and highly electronically conductive polymers (Kassi et al. 2011), and thus has the potential to replace oil-based chemicals such as methacrylic acid, fumaric acid, maleic acid and acrylic acid. Because of this versatility, the demand for IA is growing, and its world production is expected to reach 52,000 tons per year by 2025, with an expected market value of US\$260 million (Carvalho et al., 2018). Many chemical methods have been employed to synthesize IA, including the distillation of citric acid, carboxylation of acetylene derivatives, and isomerization of citraconic acid. However, these methods often require multiple separation steps, produce low yields, and are not economically viable because of the need for chemicals that are difficult to obtain. The use of these chemical methods has not yet led to industrial-scale production.

IA is synthesized through the decarboxylation of *cis*-aconitic acid, a citric acid cycle intermediate, by *cis*-aconitic acid decarboxylase (CAD). Although industrial-scale production of IA by fermentation of glucose by *Aspergillus terreus* has been demonstrated (Krull et al. 2017), the process has some limitations. Fermentation using *A. terreus* is very difficult to reproduce, resulting in a costly production process. The

51 branched filaments of the fungus make the broth highly viscous during fermentation, which poses a major
52 challenge for both mixing and aeration processes in conventional stirred-tank fermenters (Okabe et al.
53 2009). *A. terreus* is classified as a biosafety level 2 organism in several countries because of its potential to
54 produce toxins. Therefore, many researchers are seeking for alternative hosts for the production of IA.
55 Several potential alternative host cells for IA production, such as *Saccharomyces cerevisiae* (Young et al.
56 2018), *Corynebacterium glutamicum* (Otten et al. 2015), *Yarrowia lipolytica* (Zhao et al. 2019), *Ustilago*
57 *maydis* (Geiser et al., 2016) and *Pichia kudriavzevii* (Sun et al. 2020) have been investigated. Harder et al.
58 reported the production of 32 g/L IA in engineered *E. coli* (Harder et al., 2016), which constitutes a major
59 milestone in IA production. In all strains, the IA production were lower than that of *A. terreus*. It is therefore
60 a challenge to find a host organism which can express the CAD at higher levels, and thus increase IA
61 biosynthesis.

62 Fission yeast (*Schizosaccharomyces pombe*) is one of the most useful model organisms. Its complete
63 genome sequence was determined in 2002 (Wood et al. 2002). *S. pombe* has genetic features more similar
64 to higher eukaryotes than those of the classical model organism *S. cerevisiae*, including the presence of
65 introns in about half of its genes, and is therefore a well-studied model organism for genetic and physiologic
66 research (Hoffman et al. 2015). *S. pombe* can be easily manipulated in the laboratory, grows quickly, and
67 does not show pathogenicity, making it an excellent host for the production of material such as ricinoleic
68 acid (Yazawa et al. 2013) and punicic acid (Garaiova et al. 2017). Acid-tolerant yeasts have the advantage
69 direct organic acid production such as lactic acid (Ozaki et al. 2017) and 3-hydroxypropionic acid (Suyama
70 et al. 2017; Takayama et al. 2018). *S. pombe* is naturally tolerant to 3-HP and shows high growth even in
71 the presence of 50 g/L 3- hydroxypropionic acid (Kildegaard et al. 2014). It may be possible to
72 metabolically engineer *S. pombe* to produce several kinds of organic acid. In this study, we demonstrate a
73 strategy for the metabolic engineering of *S. pombe* for IA production from a renewable resource, and
74 demonstrate the potential of *S. pombe* as a host for the production of value-added chemicals. Three
75 approaches were used: 1) relocation of CAD enzymes to the cytosol or mitochondria, 2) deletion of several
76 TCA cycle enzymes and transporters in the mitochondria, and 3) cultivation at increased cell density. These
77 strategies increased the production of IA to 1.555 g/L, a value which was twelve-fold higher than that of a
78 strain simply expressing cytosolic CAD.

2. Materials and methods

2.1 Strains and media

Table 1 contains all strains used in this study. The parental strain *S. pombe* FY12804 is available in NBRP-Yeast, Japan. YM medium (BD Diagnostic Systems, Sparks, MD, USA) or EMM medium (Formedium, Norfolk, United Kingdom) were used for yeast cultivation.

2.2 Construction of plasmids and homologous recombination (HR) donors

Table 1 contains all plasmids used in this study. The primers used in this study are listed in Table S1. The plasmid pMZ374, expressing Cas9 and gRNA (Jacobs et al. 2014), was purchased from Addgene (Watertown, MA). A 20-base along with the NGG PAM sequence (N20NGG) in the *S. pombe* genome was designed using CHOPCHOP (<https://chopchop.cbu.uib.no/>). The sequences of HR donor about 500 bp homology arms upstream and downstream of the Cas9 digestion were selected.

A Cas9 protein expression plasmid targeting the *idh2* gene (GenBank accession number NM_001021109) was created using the KOD-Plus-mutagenesis Kit (TOYOBO, Co. Ltd. Osaka, Japan) according to the manufacturer's instructions. A template pMZ374 was used with the primer pair fw-idh2-Cas9-inv/rev-idh2-Cas9-inv. The resulting plasmid was named pMZ374-*idh2*. Other plasmids for Cas9 targeting were summarized in Table 1. They were constructed in a similar way.

To construct a gene expression cassette, we used the plasmid pDUAL-hsp (Ozaki et al. 2017) as a vector. Plasmid pDUAL-hsp_CAD was constructed as follows. A fragment was amplified with the primer pairs fw-hsp_CAD-insert/rev-hsp_CAD-insert using a codon-optimized CAD gene (DDBJ accession number LC702899) fragment as a template. Then the fragment was ligated into the *Xho*I and *Sac*I sites of pDUAL-hsp. To create HR donor for integration of the CAD into the chromosomal *idh2* region, the CAD expression cassette (Phsp-CAD-Tnmt1) was produced using PCR with the primer pair fw-idh2-knock_in-3/rev-idh2-knock_in-4. Upstream and downstream regions were amplified with the primer pairs fw-idh2-knock_out-1/rev-idh2-knock_in-2 and fw-idh2-knock_in-5/rev-idh2-knock_out-4, respectively. The three amplified fragments were combined using overlap extension PCR with the primer pair fw-idh2-knock_out-1/rev-idh2-knock_out-4. Other HR donor DNAs were made similarly; these are summarized in Table 1.

To construct HR donor for disruption of the *idh2* gene, the upstream and downstream regions were amplified with the primer pairs fw-*idh2*-knock_out-1/rev-*idh2*-knock_out-2 and fw-*idh2*-knock_out-3/rev-*idh2*-knock_out-4, respectively. To obtain the chromosomal *idh2* region disrupting HR donor, the two fragments were combined using overlap extension PCR with the primer pair fw-*idh2*-knock_out-1/rev-*idh2*-knock_out-4. Other HR donor DNAs were constructed in the same way.

For construction of the *mfsA* expression plasmid, the codon-optimized *mfsA*-encoding gene from *A. terreus* (DDBJ accession number LC702900) was amplified using PCR with synthetic oligonucleotides (Invitrogen, Carlsbad, CA, USA) as the template, with the primer pair fw-pDUAL-FFH61_*mfsA*-insert/rev-pDUAL-FFH61_*mfsA*-insert. The PCR product was ligated into pDUAL-FFH61 (RIKEN Bioresource Research Center; <https://web.brc.riken.jp/en/>) with the *NheI/SalI*, and the resulting plasmid was named pDUAL-FFH1_*mfsA*. Plasmids expressing *mce1* (GenBank accession number NM_001019849), *aco1ΔMTS* (GenBank accession number NM_001019456), *mpc1* (GenBank accession number NM_001022732), *mpc2* (GenBank accession number NM_001018247), *cit1* (GenBank accession number NM_001019149), and *pyr1* (GenBank accession number NM_001021807) were constructed using *S. pombe* genome as template DNA. The plasmids were constructed in the same way as that described above, and are summarized in Table 1.

To construct a CAD gene fused with the mitochondrial targeting sequence, the mitochondrial targeting sequence of the *S. pombe* endogenous *aco2* gene (GenBank accession number NM_001022108) was amplified using the primer pair fw-hsp_mt-CAD-insert-up-1/rev-hsp_mt-CAD-insert-down-2 using the *S. pombe* genome as a template. The CAD gene was amplified using the primer pair fw-hsp_mt-CAD-insert-up-3/rev-hsp_CAD-insert with the plasmid pDUAL-hsp_CAD as a template. The two amplified fragments were conjugated by overlap extension PCR using the primer pair fw-hsp_mt-CAD-insert-up-1/rev-hsp_CAD-insert. The resulting DNA was cloned into the pDUAL-hsp, plasmid as described above.

2.3 Genome editing

All genome editing experiments were carried out using the lithium acetate method (Gietz et al. 2007) by co-transformation of the pMZ374 or its derivatives with the respective HR donor fragments. Before transformation, the cells were incubated overnight at 30°C with shaking at 220 rpm in test tubes

with 5 mL of YM medium. This starter culture was used to inoculate 50 mL of YM medium at an initial OD₆₀₀ of 0.3. The cells were grown to an OD₆₀₀ of 0.6, or for approximately six hours; cells were then transformed using the lithium acetate method. EMM plates containing with 225 mg/L leucine were used for the selection of transformants, and grown at 30°C for approximately seven days. Transformants were verified using colony PCR and DNA sequencing. The overexpressed genes *mce1*, *aco1ΔMTS*, *mfsA*, *mpc1*, *mpc2*, *cit1*, and *pyr1* were transformed by complementation of a leucine auxotroph with a *leu* marker expressed under the control of an *efla-c* constitutive promoter.

2.4 Culture conditions

For IA fermentation, strains were pre-cultured in 5 mL of YM medium for 24 hours at 30°C and then washed once with distilled water. This starter culture was used to inoculate 5 mL of EMM medium containing with 225 mg/L each of uracil and leucine at an initial OD₆₀₀ of 0.3. The resulting cultures were incubated at 30°C with shaking at 220 rpm, and samples were taken at the indicated time points.

2.5 Analytical methods

Cell growth was evaluated by measuring the OD at 600 nm using a UVmini-1240 spectrophotometer (Shimadzu Corporation, Kyoto, Japan). After centrifugation at 10,000 rpm for 10 min, the supernatant was diluted appropriately before HPLC analysis. Residual glucose was analyzed using a Prominence HPLC System (Shimadzu) equipped with a Shodex SUGAR KS-801 column (6 μm, 300 mm × 8.0 mm; Shodex, München, Germany). The mobile phase was distilled water at a flow rate of 0.8 mL/min. The peak was monitored using a conductivity detector.

IA was analyzed using an HPLC equipped with a SCR-102H column (7 μm, 8.0 mm ID × 300 mm; Shimadzu). *p*-Toluenesulfonic acid (5 mM) was used as the mobile phase. A conductivity detector was used for peak monitoring. IA standards (Nacalai Tesque, Kyoto, Japan) were used to detect and quantify IA in metabolites.

3. Results

3.1 Tolerance test with IA in *S. pombe*

S. pombe has been employed as a host cell for the production of organic acids such as lactic acid (Ozaki et al. 2017) and 3-hydroxypropionic acid (Takayama et al. 2018). IA tolerance in *S. pombe* has not yet been studied. Tolerance tests were performed using *S. pombe* FY12804 *ku70*Δ strain at 30°C in EMM medium. *S. pombe* cells were exposed to 0, 5, 10, 15, or 20 g/L of IA showed a dose-dependent cell growth inhibition. Fig. 1 shows that the values of OD₆₀₀ after 72 hours of cultivation without pH control. The values of OD₆₀₀ with 15 g/L of IA was about 69.6% lower than that of the control without IA. We also carried out tolerance tests using *S. cerevisiae* strain MYA1108 in SD medium. Dose-dependent growth of *S. cerevisiae* was also observed. However, in the presence of 15 g/L IA, the *S. cerevisiae* strain did not show any cell growth. The values of pKa (IA) is 3.85, which is almost same as pKa of lactic acid (3.86). The pH at IA-containing defined mineral medium was 4. These results indicate that *S. pombe* has high tolerance to IA including inhibition effects of deprotonated form compared to *S. cerevisiae*, and thus could be potentially metabolically engineered to produce IA.

3.2 IA production in the *S. pombe* cytosol by CAD overexpression

The natural IA producer *A. terreus* has a *cis*-aconitate decarboxylase (CAD) gene, which produces the enzyme needed to synthesize IA from *cis*-aconitate (Bonnarme et al. 1995; Kanamasa et al. 2008). In this study, a codon-optimized CAD gene from *A. terreus* under the control of an *hsp* promoter was integrated into the protease-encoding *isp6* locus (GenBank accession number NM_001019245) using the CRISPR-Cas9 system (Jacobs et al. 2014). Previous studies have suggested that protein expression in *S. pombe* is improved in strains lacking intracellular proteases (Idiris et al. 2010), and we hypothesized that this system may enhance the production of IA. However, no IA was detected after the cultivation of the strain ATR5-*isp6*Δ::CAD. We added *cis*-aconitate to the medium in an attempt to improve the precursor supply, but this addition did not produce IA, and *cis*-aconitate was not consumed (data not shown).

Aconitase catalyzes the reversible isomerization of citrate and isocitrate via *cis*-aconitate. We assumed that the active TCA cycle consumes *cis*-aconitate, and we therefore disrupted isocitrate dehydrogenase gene *idh2*, which converts isocitrate to α-ketoglutarate. *S. pombe* has two *idh* isozyme (*idh1*

and *idh2*) and deleting either *idh* gene was not lethal (Kim et al. 2010). We constructed a strain, ITA1, which is an *idh2*-deficient ATR5-*isp6*Δ::CAD strain. ITA1 successfully produced 0.134 g/L of IA from 50 g/L of glucose after 72 hours of cultivation (Fig. 2). Some of the aconitate hydratase produced by *S. pombe* was reported to be localized in the cytosol (Jung et al. 2015). To increase the availability of cytosolic citrate, we overexpressed a mitochondrial citrate exporter *mce1* gene in ITA1, and the resulting strain was named ITA1-m. The production of IA was only slightly improved, reaching 0.153 g/L (Fig. 2). We also generated a strain overexpressing an IA transporter gene, *mfsA*, (Li et al. 2011; Sraat et al. 2014) under the *eflA-c* promoter. This transporter is known to export IA into the medium in *S. cerevisiae* (Young et al. 2018) and *A. niger* (Steiger et al., 2016; Li et al. 2011). In the resulting strain, ITA1-mm, IA production was slightly increased to 0.206 g/L (Fig. 2). A genome-wide analysis indicated that *aco1* was mainly localized in the mitochondria (Jung et al. 2015). We constructed *aco1*ΔMTS, which lacks its mitochondrial targeting sequence, and overexpressed *aco1*ΔMTS in ITA1-m. However, this strain did not show significant increase in IA production. Since there was no significant increase in the expression of the gene for IA production in the cytosol, we attempted to construct a mitochondrial IA production pathway in *S. pombe*.

3.3 IA production in *S. pombe* mitochondria with MTS-fused CAD expression

Fig. 3a shows the IA production pathway with mitochondrially localized CAD. Most eukaryotes have mitochondria as one of their organelles, and proteins localized in the mitochondria generally contain a mitochondrial targeting sequence (MTS) at their N-termini. The mitochondrial outer membrane recognizes the MTS, and the proteins are transported into the mitochondria, in which these proteins function appropriately. The fission yeast *S. pombe* has two genes encoding aconitase, *aco1* (SPAC24C9.06c) and *aco2* (SPBP4H10.15). *aco1* has an MTS consisting of 21 amino acids, and *aco2* has an MTS consisting of 50 amino acids. We designed mitochondrially localized CAD by fusing *aco1*MTS or *aco2*MTS to the N-terminus of CAD. These two genes were integrated into the *idh2* locus and expressed under the *hsp* promoter. Although *aco1*MTS-fused CAD overexpression did not contribute to IA production (data not shown), the *aco2*MTS-fused CAD (named mt-CAD) expressing strain produced 0.438 g/L of IA from 50 g/L of glucose after 72 hours of cultivation, a titer that was about four times higher than that of ITA1 (Fig. 3b). This observation suggests that CAD expression in mitochondria is suitable for IA production in *S. pombe*. The resulting strain was named ITA2 and used in the following experiments.

3.4 Enhancement of precursor supply by gene overexpression or repression of the downstream pathway

Using strain ITA2, we tried to enhance the upstream pathway of *cis*-aconitate synthesis by overexpressing the relevant genes. MPC1 and MPC2 are proteins that transport cytosolic pyruvate into the mitochondria (Herrero et al. 2016). A pyruvate lyase, *pyr1*, that converts pyruvate to oxaloacetate, and a citrate synthase, *cit1*, that converts oxaloacetate to citrate may enhance the TCA cycle in mitochondria. However, overexpression of these genes reduced IA production compared to ITA2 (Fig. 3b). These results indicate that the upstream pathway to the mitochondria was not the rate-limiting step, and we therefore focused on suppressing the downstream pathway and improving the availability of citrate in the mitochondria. We disrupted the *kgd3* (SPAC16E8.17c) gene, which encodes succinate-CoA ligase, which converts 2-oxoglutarate to succinate; or a gene, *mdh1*, encoding malate dehydrogenase, which converts malate to oxaloacetate. However, no improvements were observed in these deletion strains (Fig. 3b).

3.5. Disruption of transporters and *acl2* improved IA production

S. pombe has the *mae1* gene (GenBank accession number NM_001018643), which encodes a permease for several C4 dicarboxylic acids. To prevent the leakage of carbon flux from TCA cycle and improve IA production, the gene *mae1* encoding a malate/succinate exporter was deleted. The resulting strain produced 0.475 g/L of IA after 72 hours of cultivation, a slightly higher titer than that produced by ITA2 (Fig. 3b). *S. pombe*, unlike *S. cerevisiae*, has genes encoding the ATP citrate lyase (GenBank accession number; *acl1*; NM_001022121 and *acl2*; NM_001018643). Generally, oleaginous yeast species carry *acl* genes, to permit the accumulation of high levels of cytoplasmic acetyl-CoA derived from mitochondrial citrate (Zhou et al. 2012). To improve the citrate level in the mitochondria, we disrupted the gene *acl2*, which encodes citrate lyase, that converts cytosolic citrate to oxaloacetate. As seen in Fig. 3b, the *acl2*-deleted strain produced 0.581 g/L of IA after 72 hours of cultivation. The double mutant, in which both *acl2* and *mae1* were deleted, produced 0.737 g/L of IA, a 1.7-fold higher titer than that of ITA2. A small amount of citrate was produced in all strains (less than 0.25 g/L). Malate was not detected in all strains, and less than 0.1 g/L of succinate was detected in all strains except the *mae1* deletion strain. Although we introduced an additional copy of mt-CAD, the IA production of the resulting strain, named ITA3, was not improved. This observation suggests that CAD activity was not rate-limiting, and more efforts should be made to increase precursor availability. We constructed strain ITA4, in which the transporter gene *mce1* encoding

the mitochondrial membrane protein that exports mitochondrial citrate to the cytosol (Kadooka et al. 2019) was deleted from ITA3. The IA production of ITA4 was increased by up to 1.110 g/L of IA after 72 hours of cultivation (Fig. 3b), a titer which was 1.4-fold higher than that of ITA3.

3.6 Increased cell density cultivation to recover cell growth and improve IA production

The time courses of IA production, cell growth, and sugar consumption of the ITA3 and ITA4 strains are shown in Fig. 4a. Although ITA4 produced more IA than ITA3 after 72 hours of fermentation, the cell growth of ITA4 was significantly decreased in minimal medium compared to that of ITA3 (Fig. 4b). The OD₆₀₀ value of ITA3 reached 8.3 after 48 hours of cultivation, while that of ITA4 was only 3.2 after 72 hours of cultivation. As shown in Fig. 4c, the glucose consumption of ITA4 was also significantly slower than that of ITA3. To recover the cell growth, we added citrate to the culture medium. However, no improvement in cell growth was observed (data not shown). We tried to optimize the appropriate initial OD for IA production using strain ITA4. Increased cell density cultivation is effective in microbial fermentation. Because it can shorten the cultivation time, and the carbon source that was used for cell growth can be used for bioproduction (Westman et al. 2015). When the initial OD was 3.0, the production of IA was increased and reached 1.555 ± 0.010 g/L (Fig. 4d). ITA3 produced 0.992 g/L of IA after 24 hours, and production did not increase thereafter (Fig. 4d). The cell growth of ITA4 reached 6.3 after 72 hours, and glucose was consumed efficiently after cultivation (Fig. 4e,4f). In contrast, ITA3 had completely consumed the glucose after 24 hours, and cell growth was slightly improved.

4. Discussion

In this study, we aimed to develop a microbial pathway for the biosynthesis of IA by metabolic engineering of *S. pombe*. The cytosolic expression of enzymes related to IA synthesis failed to increase IA production (Fig. 2), and mitochondrial localization of the enzymes was necessary for IA production (Fig. 3b). Deletions of the TCA cycle enzymes, except *idh2*, had negative effects on IA production, and inactivation of some transporters were effective in increasing IA production in *S. pombe*. Cultivation with an initial high cell density led to the production of up to 1.555 g/L of IA production, which is highest observed using *S. pombe* as a host.

Various strategies have been used in attempts to efficiently synthesize IA from *cis*-aconitate: strategies to

transport *cis*-aconitate out of the mitochondria (Zhao et al. 2019); to convert *cis*-aconitate to *trans*-aconitate according to natural metabolic process to IA in *Ustilago maydis* without competition with the TCA cycle (Geiser et al. 2016); and to introduce a linker between aconitase and CAD (Xie et al. 2020). In this study, we aimed to achieve high IA production by localizing CAD to the mitochondria. Mitochondrial localization is one way to maximize the availability of TCA cycle intermediates (Zhang et al. 2019). Mitochondrial targeting of CAD in *A. niger* lead to higher titers (Blumhoff et al., 2013). We prepared codon-optimized the CAD gene for *S. pombe* and attached the MTS of endogenous *aco2* to the 5' end of the CAD gene, constructing mt-CAD, and overexpressed it under the *hsp* promoter (ITA2). We succeeded in increasing the IA production by more than three-fold compared to that of ITA1 (Fig. 3b). This increase was caused by a high concentration of *cis*-aconitate in the mitochondria, and the efficiency of conversion from *cis*-aconitate to IA was increased. This method may be applied to the microbial production of other high value-added compounds derived from TCA cycle intermediates.

When we need the intermediates of the TCA cycle to be accumulated, the distribution between the increase in carbon flux to the target material and that to cell growth must be appropriately balanced. In *S. cerevisiae*, disruption of *sdh2*, *sdh1*, *idh1*, and *idp1* increased the production of succinate (Raab et al. 2010). Disruption of *frdBC* (succinate dehydrogenase) and *fumABC* (fumarate hydratase) increased 2-oxoglutarate production in *E. coli* (Chen et al. 2020). We attempted to disrupt TCA cycle-related genes to increase the carbon flux to IA. Although the deletion of *kgd3* and *mdh1* did not improve the IA titer, the deletion of *mae1* increased IA production. MAE1p is used as an exporter of succinate, fumarate, and malate from the mitochondria (Kang et al. 2021). The deletion of *mae1* contributes to the prevention of carbon flux leakage from the TCA cycle. Disruption of *acl2*, which catalyzes the formation of acetyl-CoA and oxaloacetate from citrate (Chu et al. 2010) causes decline in the concentration of cytosolic oxaloacetate, and reduces the citrate antiport activity (Kadooka et al. 2019). Therefore, the citrate concentration in the mitochondria increased, which may have contributed to the improvement of IA biosynthesis.

Since increasing the copy number of mt-CAD did not significantly increase IA production (Fig. 3b), we made an effort to suppress the consumption of citrate, to further increase IA production. The IA production of the *mce1*-disrupted strain ITA4 was higher than that of ITA3 in minimal medium (Fig. 4a). However, disruption of *mce1* resulted in a significant decrease in cell growth (Fig. 4b). Chen et al. reported the cell

growth of *mce1*-disrupted strain was recovered in media other than minimal medium (Chen et al. 2014). Therefore, we cultured ITA4 strain in several media: YM, YPD, and minimal medium containing 1.0 g/L yeast extract. Although cell growth was restored in these media, the IA titer was not improved (data not shown). Malecki et al. reported that the disruption of *mce1* causes inactivation of the lysine biosynthesis pathway in *S. pombe*, and lysine addition improves its cell growth (Malecki et al. 2016). However, there was no increase in cell growth or IA production with the addition of lysine to the medium (data not shown). In order to promote cell growth and activate IA production, increased-cell density cultivation was used with the ITA4 strain in minimal medium. When the initial OD was set at 3.0, the OD after 72 hours reached as high as 6.3, and the IA titer was markedly improved, to about 1.5 times higher than that of strain ITA3. Further investigation into culture conditions may improve the production of IA in this strain.

5. Conclusion

We succeeded in constructing a mitochondrial IA biosynthesis pathway in *S. pombe* using the CRISPR-Cas9 genome editing system. We found that deletion of the genes *idh2*, *mae1*, *acl2*, and *mce1* was effective for increasing IA production. By using increased cell density cultivation with the mutant strains, we succeeded in producing 1.555 g/L of IA, which was the highest value obtained using *S. pombe* as a host, and about 11 times higher than that of the starting stain. This study demonstrates the potential of *S. pombe* as a host for the production of engineered material, and we believe that the establishment of the IA production process can serve as an effective platform technology for the synthesis of derivatives of other TCA cycle intermediates.

6. Acknowledgements

This work was supported by the Japan Society for the Promotion of Science (JSPS) Grant-in-Aid for Scientific Research (B) (Grant Number 19H02526), Japan (to T.T.). The authors would like to thank Enago (www.enago.jp) for the English language review.

CRedit authorship contribution statement

N.F. and T.T. conceived and designed research. N.F., M.I., M.K., Y.H. conducted experiments. A.K. contributed new reagents or analytical tools. N.F. and T.T. analyzed data and wrote the manuscript. All authors read and approved the manuscript.

Declaration of Competing Interest

The authors declare that they have no known competing financial interests or personal relationships that could have appeared to influence the work reported in this paper.

References

- Bonnarme P, Gillet B, Sepulchre AM, Role C, Beloeil JC, Ducrocq C (1995) Itaconate biosynthesis in *Aspergillus terreus*. J Bacteriol 177:3573–3578. doi:[10.1128/jb.177.12.3573-3578.1995](https://doi.org/10.1128/jb.177.12.3573-3578.1995)
- Blumhoff ML, Steiger MG, Mattanovich D, Sauer M. (2013) Targeting enzymes to the right compartment: metabolic engineering for itaconic acid production by *Aspergillus niger*. Metab Eng. 2013;19:26-32. doi:10.1016/j.ymben.2013.05.003
- Chen JS, Beckley JR, McDonald NA, Ren L, Mangione M, Jang SJ, Elmore ZC, Rachfall N, Feoktistova A, Jones CM, Willet AH, Guillen R, Bitton DA, Bähler J, Jensen MA, Rhind N, Gould KL (2014) Identification of new players in cell division, DNA damage response, and morphogenesis through construction of *Schizosaccharomyces pombe* deletion strains. G3 (Bethesda) 5:361–370. doi:[10.1534/g3.114.015701](https://doi.org/10.1534/g3.114.015701)
- Chen X, Dong X, Liu J, Luo Q, Liu L (2020) Pathway engineering of *Escherichia coli* for α -ketoglutaric acid production. Biotechnol Bioeng 117:2791–2801. doi:[10.1002/bit.27456](https://doi.org/10.1002/bit.27456)
- Chu KY, Lin Y, Hendel A, Kulpa JE, Brownsey RW, Johnson JD (2010) ATP-citrate lyase reduction mediates palmitate-induced apoptosis in pancreatic beta cells. J Biol Chem 285:32606–32615. doi:[10.1074/jbc.M110.157172](https://doi.org/10.1074/jbc.M110.157172)
- de Carvalho JC, Magalhães AI Jr CR (2018) Soccol Biobased itaconic acid market and research trends - is it really a promising chemical? Chimica Oggi - Chemistry Today 36:56–58

342 Deng S, Dai Z, Swita M, Pomraning KR, Hofstad B, Panisko E, Baker S, Magnuson J (2020) Deletion
 343 analysis of the itaconic acid biosynthesis gene cluster components in *Aspergillus*
 344 *pseudoterreus* ATCC32359. Appl Microbiol Biotechnol 104:3981–3992. doi:[10.1007/s00253-020-10418-](https://doi.org/10.1007/s00253-020-10418-0)
 345 [0](https://doi.org/10.1007/s00253-020-10418-0)

346 Garaiova M, Mietkiewska E, Weselake RJ, Holic R (2017) Metabolic engineering of
 347 *Schizosaccharomyces pombe* to produce punicic acid, a conjugated fatty acid with nutraceutic properties.
 348 Appl Microbiol Biotechnol 101(21):7913–7922. doi: 10.1007/s00253-017-8498-8.

349 Geiser E, Przybilla SK, Friedrich A, Buckel W, Wierckx N, Blank LM, Bölker M (2016) *Ustilago maydis*
 350 produces itaconic acid via the unusual intermediate *trans*-aconitate. Microb Biotechnol 9:116–126.
 351 doi:[10.1111/1751-7915.12329](https://doi.org/10.1111/1751-7915.12329)

352 Gietz RD, Schiestl RH (2007) High-efficiency yeast transformation using the LiAc/SS carrier DNA/PEG
 353 method. Nat Protoc 2:31–34. doi:[10.1038/nprot.2007.13](https://doi.org/10.1038/nprot.2007.13)

354 Harder B-J, Bettenbrock K, Klamt S (2016) Model-based metabolic engineering enables high yield
 355 itaconic acid production by *Escherichia coli*. Metab Eng 38:29–37. doi:[10.1016/j.ymben.2016.05.008](https://doi.org/10.1016/j.ymben.2016.05.008)

356 Herrero J, Muffato M, Beal K, Fitzgerald S, Gordon L, Pignatelli M, Vilella AJ, Searle SM, Amode R,
 357 Brent S, Spooner W, Kulesha E, Yates A, Flicek P (2016) Ensembl comparative genomics
 358 resources. Database (Oxford) 2016:bav096. doi:[10.1093/database/bav096](https://doi.org/10.1093/database/bav096)

359 Hoffman CS, Wood V, Fantes PA (1 Oct. 2015) An Ancient Yeast for Young Geneticists: A Primer on
 360 the *Schizosaccharomyces pombe* Model System. Genetics 201:403–423. doi:[10.1534/genetics.115.181503](https://doi.org/10.1534/genetics.115.181503)

361 Idiris A, Tohda H, Sasaki M, Okada K, Kumagai H, Giga-Hama Y, Takegawa K (2010) Enhanced protein
 362 secretion from multiprotease-deficient fission yeast by modification of its vacuolar protein sorting
 363 pathway. Appl Microbiol Biotechnol 85:667–677. doi:[10.1007/s00253-009-2151-0](https://doi.org/10.1007/s00253-009-2151-0)

364 Jacobs JZ, Ciccaglione KM, Tournier V, Zaratiegui M (2014) Implementation of the CRISPR-Cas9
 365 system in fission yeast. Nat Commun 5:5344. doi:[10.1038/ncomms6344](https://doi.org/10.1038/ncomms6344)

366 Jung SJ, Seo Y, Lee KC, Lee D, Roe JH, Daeyoung and Roe (2015) Essential function of Aco2, a fusion
 367 protein of aconitase and mitochondrial ribosomal protein bL21, in mitochondrial translation in fission
 368 yeast. FEBS Lett 589:822–828. doi:[10.1016/j.febslet.2015.02.015](https://doi.org/10.1016/j.febslet.2015.02.015)

369 Kadooka C, Izumitsu K, Onoue M, Okutsu K, Yoshizaki Y, Takamine K, Goto M, Tamaki H, Futagami T
 370 (2019) Mitochondrial citrate Transporters CtpA and YhmaA Are Required for extracellular citric acid
 371 Accumulation and Contribute to cytosolic acetyl coenzyme A Generation in *Aspergillus luchuensis* mut.
 372 *kawachii*. Appl Environ Microbiol 85:e03136-18. doi:[10.1128/AEM.03136-18](https://doi.org/10.1128/AEM.03136-18)

373 Kanamasa S, Dwiarti L, Okabe M, Park EY (2008) Cloning and functional characterization of the cis-
 374 aconitic acid decarboxylase (CAD) gene from *Aspergillus terreus*. Appl Microbiol Biotechnol 80:223–
 375 229. doi:[10.1007/s00253-008-1523-1](https://doi.org/10.1007/s00253-008-1523-1)

376 Kang NK, Lee JW, Ort DR, Jin YS (2021) L-malic acid production from xylose by engineered
 377 *Saccharomyces cerevisiae*. Biotechnol J 17:e2000431. doi:[10.1002/biot.202000431](https://doi.org/10.1002/biot.202000431)

378 Kassi E, Loizou E, Porcar L, Patrickios, Di CS (2011) Di(n-butyl) itaconate end-functionalized polymers:
 379 synthesis by group transfer polymerization and solution characterization. Eur Polym J 47:816–822.
 380 doi:[10.1016/j.eurpolymj.2010.09.011](https://doi.org/10.1016/j.eurpolymj.2010.09.011)

381 Kildegaard KR, Hallström BM, Blicher TH, Sonnenschein N, Jensen NB, Sherstyk S, Harrison SJ, Maury
 382 J, Herrgård MJ, Juncker AS, Forster J, Nielsen J, Borodina I (2014) Evolution reveals a glutathione-
 383 dependent mechanism of 3-hydroxypropionic acid tolerance. Metab Eng 26:57-66. doi:
 384 [10.1016/j.ymben.2014.09.004](https://doi.org/10.1016/j.ymben.2014.09.004).

385 Kim DU, Hayles J, Kim D, Wood V, Park HO, Won M, Yoo HS, Duhig T, Nam M, Palmer G, Han S,
 386 Jeffery L, Baek ST, Lee H, Shim YS, Lee M, Kim L, Heo KS, Noh EJ, Lee AR, Jang YJ, Chung KS, Choi
 387 SJ, Park JY, Park Y, Kim HM, Park SK, Park HJ, Kang EJ, Kim HB, Kang HS, Park HM, Kim K, Song
 388 K, Song KB, Nurse P, Hoe KL (2010) Analysis of a genome-wide set of gene deletions in the fission yeast
 389 *Schizosaccharomyces pombe*. Nat Biotechnol. 28(6):617-623. doi: [10.1038/nbt.1628](https://doi.org/10.1038/nbt.1628).

390 Krull S, Hevekerl A, Kuenz A, Prüße U (2017) Process development of itaconic acid production by a
 391 natural wild type strain of *Aspergillus terreus* to reach industrially relevant final titers. Appl Microbiol
 392 Biotechnol 101:4063–4072. doi:[10.1007/s00253-017-8192-x](https://doi.org/10.1007/s00253-017-8192-x)

393 Li A, van Luijk N, ter Beek M, Caspers M, Punt P, van der Werf M (2011) A clone-based transcriptomics
 394 approach for the identification of genes relevant for itaconic acid production in *Aspergillus*. Fungal Genet
 395 Biol 48:602–611. doi:[10.1016/j.fgb.2011.01.013](https://doi.org/10.1016/j.fgb.2011.01.013)

396 Malecki M, Bitton DA, Rodríguez-López M, Rallis C, Calavia NG, Smith GC, Bähler J (2016)
 397 Functional and regulatory profiling of energy metabolism in fission yeast. Genome Biol 17:240.
 398 doi:[10.1186/s13059-016-1101-2](https://doi.org/10.1186/s13059-016-1101-2)

399 Merger F, Liebe J (1991) Preparation of 1,1-disubstituted ethylene compounds. Patent US 4:955

400 Okabe M, Lies D, Kanamasa S, Park EY (2009) Biotechnological production of itaconic acid and its
 401 biosynthesis in *Aspergillus terreus*. Appl Microbiol Biotechnol 84:597–606. doi:[10.1007/s00253-009-](https://doi.org/10.1007/s00253-009-2132-3)
 402 [2132-3](https://doi.org/10.1007/s00253-009-2132-3)

403 Otten A, Brocker M, Bott M (2015) Metabolic engineering of *Corynebacterium glutamicum* for the
 404 production of itaconate. Metab Eng 30:156–165. doi:[10.1016/j.ymben.2015.06.003](https://doi.org/10.1016/j.ymben.2015.06.003)

405 Ozaki A, Konishi R, Otomo C, Kishida M, Takayama S, Matsumoto T, Tanaka T, Kondo A (2017)
 406 Metabolic engineering of *Schizosaccharomyces pombe* via CRISPR-Cas9 genome editing for lactic acid
 407 production from glucose and cellobiose. Metab Eng Commun 5:60–67.
 408 doi:[10.1016/j.meten.2017.08.002](https://doi.org/10.1016/j.meten.2017.08.002)

409 Raab AM, Gebhardt G, Bolotina N, Weuster-Botz D, Lang C (2010) Metabolic engineering of
 410 *Saccharomyces cerevisiae* for the biotechnological production of succinic acid. Metab Eng 12:518–525.
 411 doi:[10.1016/j.ymben.2010.08.005](https://doi.org/10.1016/j.ymben.2010.08.005)

412 Steiger MG, Punt PJ, Ram AFJ, Mattanovich D, Sauer M. (2016) Characterizing MttA as a mitochondrial
 413 cis-aconitic acid transporter by metabolic engineering. *Metab Eng.* 35:95-104. doi:
 414 10.1016/j.ymben.2016.02.003.

415 Sun W, Vila-Santa A, Liu N, Prozorov T, Xie D, Faria NT, Ferreira FC, Mira NP, Shao Z (2020)
 416 Metabolic engineering of an acid-tolerant yeast strain *Pichia kudriavzevii* for itaconic acid production.
 417 *Metab Eng Commun* 10:e00124. doi:[10.1016/j.mec.2020.e00124](https://doi.org/10.1016/j.mec.2020.e00124)

418 Suyama A, Higuchi Y, Urushihara M, Maeda Y, Takegawa K (2017) Production of 3-hydroxypropionic
 419 acid via the malonyl-CoA pathway using recombinant fission yeast strains. *J Biosci Bioeng* 124:392–399.
 420 doi:[10.1016/j.jbiosc.2017.04.015](https://doi.org/10.1016/j.jbiosc.2017.04.015)

421 Takayama S, Ozaki A, Konishi R, Otomo C, Kishida M, Hirata Y, Matsumoto T, Tanaka T, Kondo A
 422 (2018) Enhancing 3-hydroxypropionic acid production in combination with sugar supply engineering by
 423 cell surface-display and metabolic engineering of *Schizosaccharomyces pombe*. *Microb Cell Fact* 17:176.
 424 doi:[10.1186/s12934-018-1025-5](https://doi.org/10.1186/s12934-018-1025-5)

425 van der Straat L, Vernooij M, Lammers M, van den Berg W, Schonewille T, Cordewener J, van der Meer
 426 I, Koops A, de Graaff LH (2014) Expression of the *Aspergillus terreus* itaconic acid biosynthesis cluster
 427 in *Aspergillus niger*. *Microb Cell Fact* 13:11. doi:[10.1186/1475-2859-13-11](https://doi.org/10.1186/1475-2859-13-11)

428 Werpy T, Petersen G (2004) Top value added chemicals from biomass. Results of Screening for Potential
 429 Candidates from Sugars and Synthesis Gas. United States I. doi:[10.2172/15008859](https://doi.org/10.2172/15008859)

430 Westman JO, Franzén CJ (2015) Current progress in high cell density yeast bioprocesses for bioethanol
 431 production. *Biotechnol J* 10:1185–1195. doi:[10.1002/biot.201400581](https://doi.org/10.1002/biot.201400581)

432 Wood V, Gwilliam R, Rajandream MA, Lyne M, Lyne R, Stewart A, Sgouros J, Peat N, Hayles J, Baker
 433 S, Basham D, Bowman S, Brooks K, Brown D, Brown S, Chillingworth T, Churcher C, Collins M,
 434 Connor R, Cronin A, Davis P, Feltwell T, Fraser A, Gentles S, Goble A, Hamlin N, Harris D, Hidalgo J,
 435 Hodgson G, Holroyd S, Hornsby T, Howarth S, Huckle EJ, Hunt S, Jagels K, James K, Jones L, Jones M,
 436 Leather S, McDonald S, McLean J, Mooney P, Moule S, Mungall K, Murphy L, Niblett D, Odell C,

437 Oliver K, O’Neil S, Pearson D, Quail MA, Rabinowitsch E, Rutherford K, Rutter S, Saunders D, Seeger
 438 K, Sharp S, Skelton J, Simmonds M, Squares R, Squares S, Stevens K, Taylor K, Taylor RG, Tivey A,
 439 Walsh S, Warren T, Whitehead S, Woodward J, Volckaert G, Aert R, Robben J, Grymonprez B, Weltjens I,
 440 Vanstreels E, Rieger M, Schäfer M, Müller-Auer S, Gabel C, Fuchs M, Düsterhöft A, Fritzc C, Holzer E,
 441 Moestl D, Hilbert H, Borzym K, Langer I, Beck A, Lehrach H, Reinhardt R, Pohl TM, Eger P,
 442 Zimmermann W, Wedler H, Wambutt R, Purnelle B, Goffeau A, Cadieu E, Dréano S, Gloux S, Lelaure V,
 443 Mottier S, Galibert F, Aves SJ, Xiang Z, Hunt C, Moore K, Hurst SM, Lucas M, Rochet M, Gaillardin C,
 444 Tallada VA, Garzon A, Thode G, Daga RR, Cruzado L, Jimenez J, Sánchez M, del Rey F, Benito J,
 445 Domínguez A, Revuelta JL, Moreno S, Armstrong J, Forsburg SL, Cerutti L, Lowe T, McCombie WR,
 446 Paulsen I, Potashkin J, Shpakovski GV, Ussery D, Barrell BG, Nurse P (2002) The genome sequence
 447 of *Schizosaccharomyces pombe*. Nature 415:871–880. doi:[10.1038/nature724](https://doi.org/10.1038/nature724)

 448 Xie H, Ma Q, Wei D, Wang F (2020) Metabolic engineering of an industrial *Aspergillus niger* strain for
 449 itaconic acid production. 3 Biotech 10:113. doi:[10.1007/s13205-020-2080-2](https://doi.org/10.1007/s13205-020-2080-2)

 450 Yazawa H, Kumagai H, Uemura H (2013) Secretory production of ricinoleic acid in fission yeast
 451 *Schizosaccharomyces pombe*. Appl Microbiol Biotechnol. 97(19):8663-8671. doi: 10.1007/s00253-013-
 452 5060-1

 453 Young EM, Zhao Z, Gielesen BEM, Wu L, Benjamin Gordon DB, Roubos JA, Voigt CA (2018) Iterative
 454 algorithm-guided design of massive strain libraries, applied to itaconic acid production in yeast. Metab
 455 Eng 48:33–43. doi:[10.1016/j.ymben.2018.05.002](https://doi.org/10.1016/j.ymben.2018.05.002)

 456 Zhang Y, Lane S, Chen JM, Hammer SK, Luttinger J, Yang L, Jin YS, Avalos JL (2019) Xylose utilization
 457 stimulates mitochondrial production of isobutanol and 2-methyl-1-butanol in *Saccharomyces cerevisiae*.
 458 Biotechnol Biofuels 12:223. doi:[10.1186/s13068-019-1560-2](https://doi.org/10.1186/s13068-019-1560-2)

 459 Zhao C, Cui Z, Zhao X, Zhang J, Zhang L, Tian Y, Qi Q, Liu J (2019) Enhanced itaconic acid production
 460 in *Yarrowia lipolytica* via heterologous expression of a mitochondrial transporter MTT. Appl Microbiol
 461 Biotechnol 103:2181–2192. doi:[10.1007/s00253-019-09627-z](https://doi.org/10.1007/s00253-019-09627-z)

Zhou J, Yin X, Madzak C, Du G, Chen J (2012) Enhanced α -ketoglutarate production in *Yarrowia lipolytica* WSH-Z06 by alteration of the acetyl-CoA metabolism. J Biotechnol 161:257–264. doi:[10.1016/j.jbiotec.2012.05.025](https://doi.org/10.1016/j.jbiotec.2012.05.025)

Figure Captions

Fig. 1 Relative cell growth after 72 hours of incubation. The orange bar on the left of each item indicates *S. pombe* strain FY12804 *ku70* Δ , and the blue bar on the right indicates *S. cerevisiae* strain MYA1108. 0, 5, 10, 15, or 20 g/L IA was added to EMM minimal medium for *S. pombe* and SD medium for *S. cerevisiae*. The data are shown as the mean and standard deviations of three independent experiments

Fig. 2 IA production after 72 hours of cultivation in EMM medium containing 50 g/L glucose using the mutant strains ITA1, ITA-m, ITA-ma, and ITA1-mm. Statistical analysis was performed using *t*-tests (two tailed; two-sample assuming equal variance; ** $p < 0.01$, * $p < 0.05$). The data are shown as the means and standard deviations of three independent experiments

Fig. 3 Engineered metabolic pathway for IA production in *S. pombe*. **a** Mitochondrial IA biosynthesis pathway from glucose in *S. pombe*. Seven genes (*pdcl01*, *pdcl02*, *l-ldh*, *adh*(SPBC337.11), *acl2*, *mce1*, *idh2*, and *mae1*, indicated in blue) were disrupted, and mt-CAD (indicated in red) was heterologously expressed. **b** IA production after 72 hours of cultivation in EMM medium containing 50 g/L glucose using mutant strains in which the following genes were overexpressed or disrupted; *mpc1-2*, mitochondrial pyruvate carrier; *cit1*, citrate synthase; *pyr1*, pyruvate carboxylase; *kgd3*, succinate-CoA ligase; *mdh1*, malate dehydrogenase; *mae1*, plasma membrane succinate fumarate malate proton symporter; *acl2*, cytosolic citrate lyase; and *mce1*, mitochondrial citrate exporter. Statistical analysis was performed using *t*-tests (two tailed; two-sample assuming equal variance; * $p < 0.05$). The data are shown as the means and standard deviations of three independent experiments

Fig. 4 Cultivation profile of strains ITA3 and ITA4 in EMM medium containing 50 g/L glucose. Time courses of IA (**a** and **d**), growth (**b** and **e**), and sugar consumption (**c** and **f**) are shown. Strain ITA3 ($OD_{init} = 0.3$) is represented by a light blue dotted line, ITA3 ($OD_{init} = 3.0$) by a blue chain line, ITA4 ($OD_{init} = 0.3$) by a light green dashed line, and ITA4 ($OD_{init} = 3.0$) by a green solid line. The data are shown as the

488 mean and standard deviations of three independent experiments

489

1

2 **Table 1** Strains and plasmids used in this study

Strain	Genotype	Source
FY12804	<i>Schizosaccharomyces pombe</i> h90 ura4-D18 leu1-32	NBRP-Yeast, Japan ^a
FY12804 <i>ku70</i> Δ	<i>Schizosaccharomyces pombe</i> h90 ura4-D18 leu1-32 <i>ku70</i> Δ	Ozaki et al. 2017
ATR5	FY12804 <i>ku70</i> Δ, <i>cdc1</i> Δ::Ptif51- <i>mhpF</i> , <i>cdc2</i> Δ::Ptif51- <i>eutE</i> , <i>l-idh</i> Δ, <i>adh</i> SPBC337.11Δ	Ozaki et al. 2017
ITA1	ATR5, <i>isp6</i> Δ::CAD, <i>idh2</i> Δ	This study
ITA1-m	ATR5, <i>isp6</i> Δ::CAD, <i>idh2</i> Δ:: <i>mce1</i>	This study
ITA1-ma	ATR5, <i>isp6</i> Δ::CAD, <i>idh2</i> Δ:: <i>mce1</i> , integration of P _{efla-c} <i>aco1</i> ΔMTS at <i>leu</i>	This study
ITA1-mm	ATR5, <i>isp6</i> Δ::CAD, <i>idh2</i> Δ:: <i>mce1</i> , integration of P _{efla-c} <i>mfsA</i> at <i>leu</i>	This study
ITA2	ATR5, <i>idh2</i> Δ::mt-CAD	This study
ITA3	ATR5, <i>idh2</i> Δ::mt-CAD, <i>mae1</i> Δ, <i>acl2</i> Δ, <i>ppp16</i> Δ::mt-CAD	This study
ITA4	ATR5, <i>idh2</i> Δ::mt-CAD, <i>mae1</i> Δ, <i>acl2</i> Δ, <i>ppp16</i> Δ::mt-CAD, <i>mce1</i> Δ	This study
Plasmid	Description	Source
pMZ374	Vector for expressing <i>adh1::cas9/rrk1::sgRNA</i> in <i>S. pombe</i> :	Addgene

	empty sgRNA target	(#59896)
pMZ374_ <i>isp6</i>	pMZ374 derivative, <i>isp6</i> sgRNA target	This study
pMZ374_ <i>idh2</i>	pMZ374 derivative, <i>idh2</i> sgRNA target	This study
pMZ374_ <i>kgd3</i>	pMZ374 derivative, <i>kgd3</i> (SPAC16E8.17c) sgRNA target	This study
pMZ374_ <i>mdh1</i>	pMZ374 derivative, <i>mdh1</i> sgRNA target	This study
pMZ374_ <i>mae1</i>	pMZ374 derivative, <i>mae1</i> sgRNA target	This study
pMZ374_ <i>acl2</i>	pMZ374 derivative, <i>acl2</i> sgRNA target	This study
pMZ374_ <i>ppp16</i>	pMZ374 derivative, <i>ppp16</i> sgRNA target	This study
pMZ374_ <i>mce1</i>	pMZ374 derivative, <i>mce1</i> sgRNA target	This study
pDUAL-hsp	Vector for constructing a gene expression cassette under hsp promoter control	Ozaki et al. 2017
pDUAL-hsp_CAD	Vector for constructing a CAD expression cassette under hsp promoter control	This study
pDUAL-hsp_mt-CAD	Vector for constructing a mt-CAD expression cassette under hsp promoter control	This study
pDUAL-FFH61	Vector under <i>ef1a-c</i> promoter control	RIKEN BRC
pDUAL-FFH61_ <i>mfsA</i>	Vector for expression of <i>mfsA</i> from <i>Aspergillus terreus</i>	This study
pDUAL-FFH61_ <i>mce1</i>	Vector for expression of <i>S. pombe</i> endogenous <i>mce1</i>	This study

pDUAL- FFH61_ <i>aco1</i> ΔMTS	Vector for expression of <i>S. pombe</i> endogenous <i>aco1</i> lacking of mitochondrial targeting sequence	This study
pDUAL- FFH61_ <i>mpc1</i>	Vector for expression of <i>S. pombe</i> endogenous <i>mpc1</i>	This study
pDUAL- FFH61_ <i>mpc2</i>	Vector for expression of <i>S. pombe</i> endogenous <i>mpc2</i>	This study
pDUAL- FFH61_ <i>cit1</i>	Vector for expression of <i>S. pombe</i> endogenous <i>cit1</i>	This study
pDUAL- FFH61_ <i>pyr1</i>	Vector for expression of <i>S. pombe</i> endogenous <i>pyr1</i>	This study

3 ^aNational Bio-Resource Project-Yeast, Japan, <https://yeast.nig.ac.jp/yeast/top.xhtml>

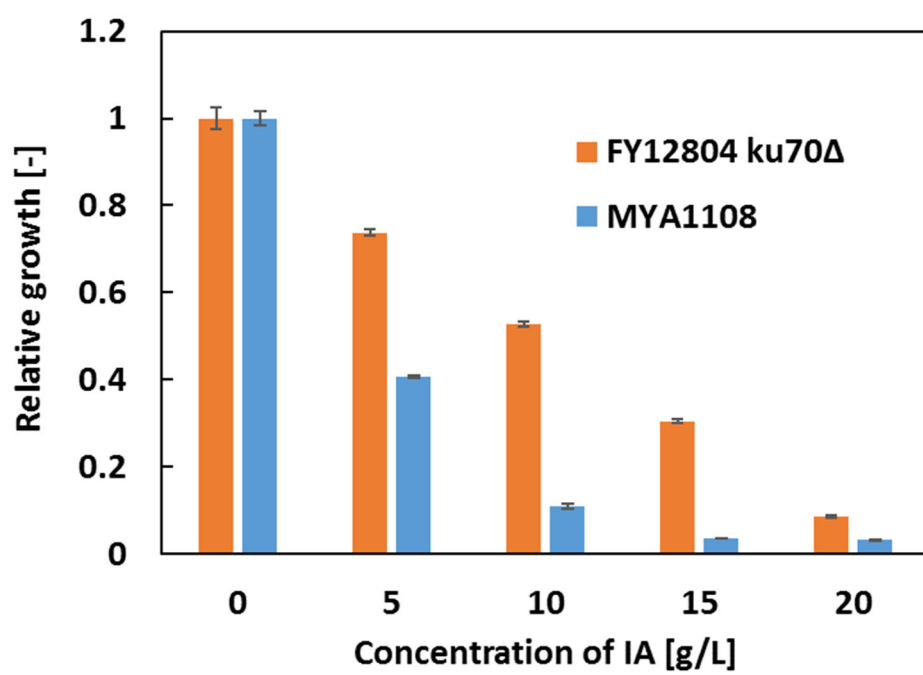


Fig. 1

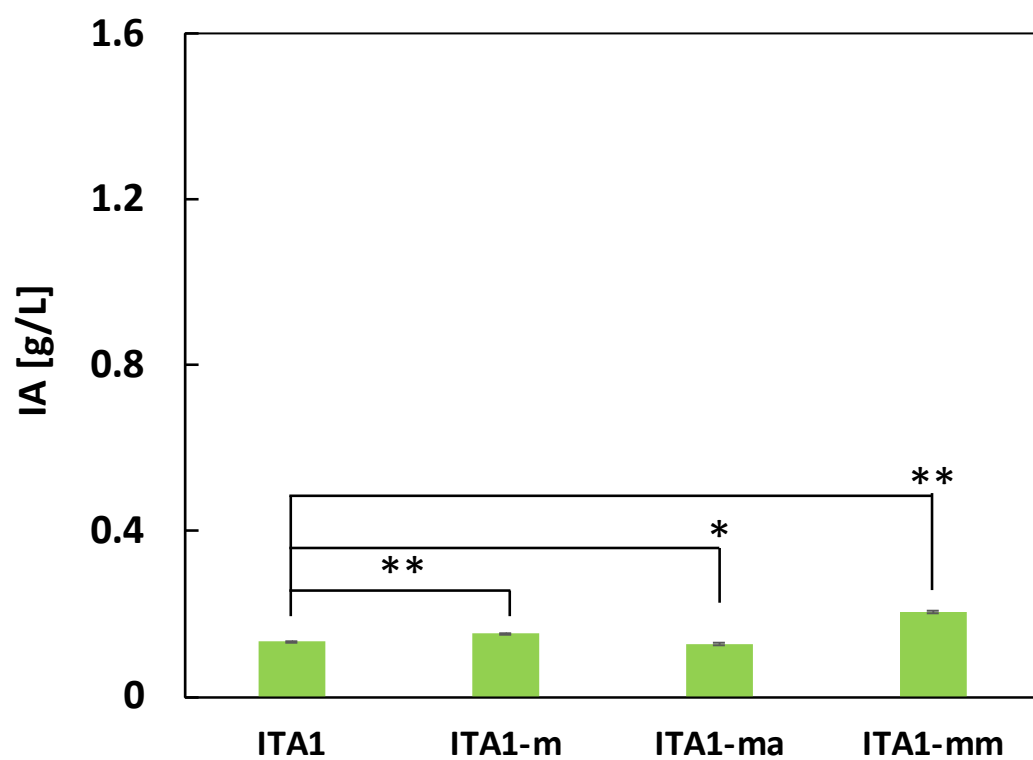


Fig. 2

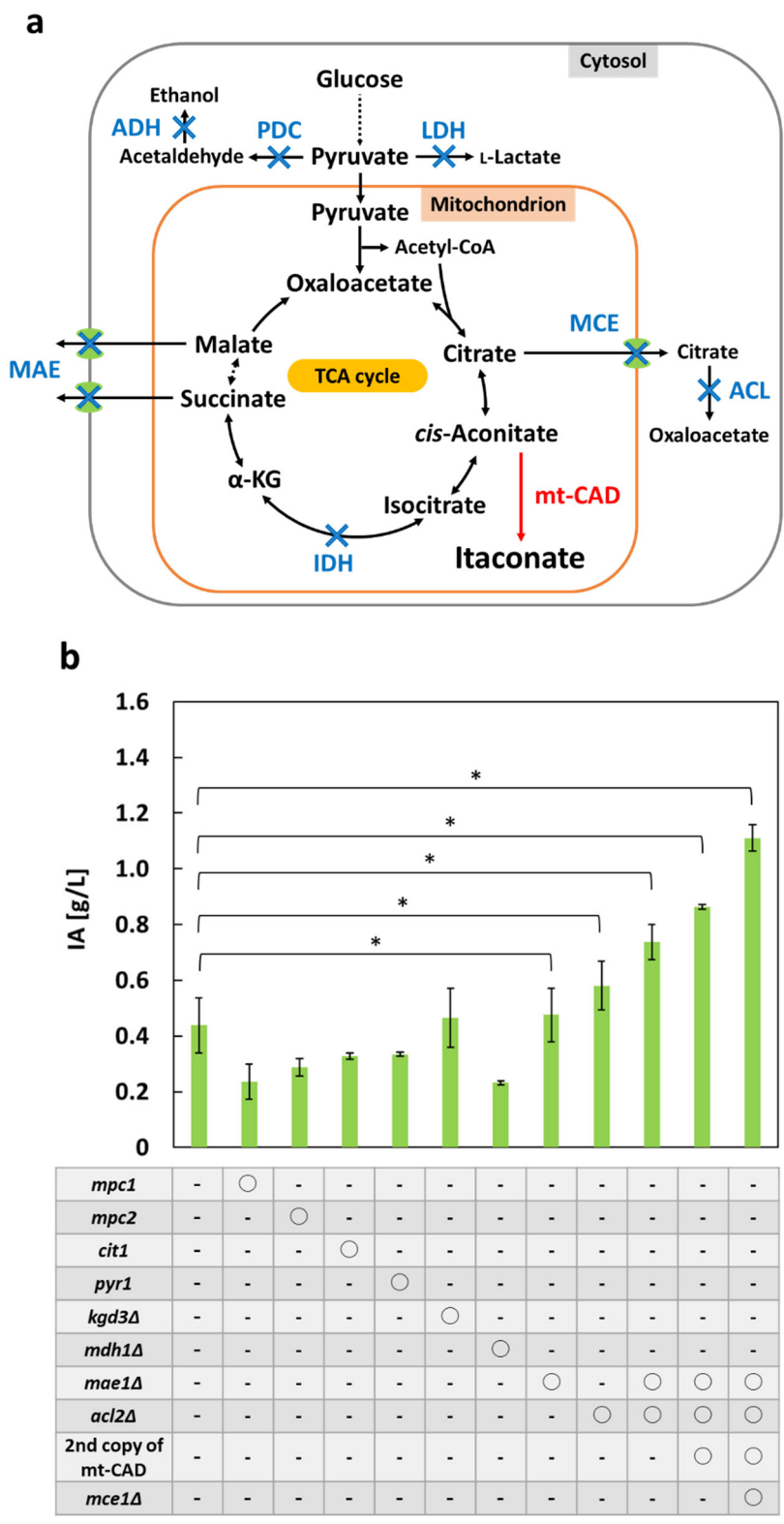


Fig. 3

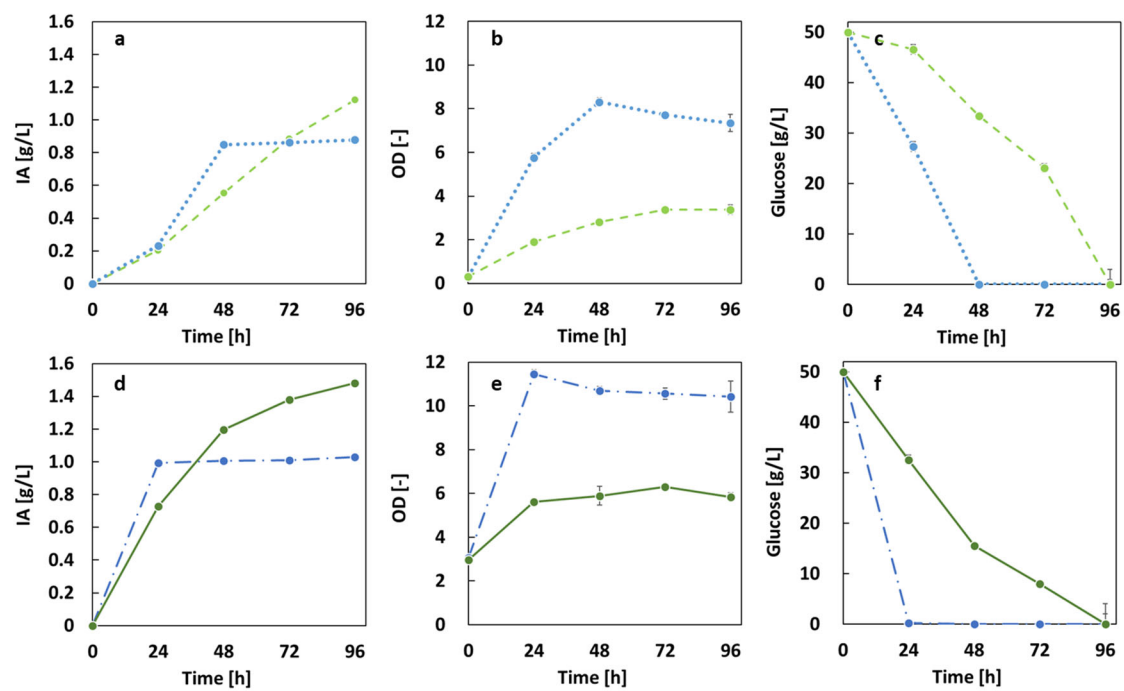


Fig. 4